Available online at www.sciencedirect.com
SCIENCE DIRECT
Geochimica et Cosmochimica Acta 70 (2006) 2902–2918
Geochimica
www.elsevier.com/locate/gca

Dual speciation of nitrogen in silicate melts at high pressure and temperature: An experimental study

Mathieu Roskosz *, Bjorn O. Mysen, George D. Cody

Geophysical Laboratory, 5251 Broad Branch Road, Washington, DC 20015, USA

Received 15 July 2005; accepted in revised form 1 March 2006

Abstract

Solubility and speciation of nitrogen in silicate melts have been investigated between 1400 and 1700 °C and at pressures ranging from 10 to 30 kbar for six different binary alkali and alkaline-earth silicate liquids and a Ca–Mg–alumino silicate. Experiments were performed in a piston–cylinder apparatus. The nitrogen source is silver azide, which breaks down to Ag and molecular N_2 below 300 °C. At high pressure and temperature, the nitrogen content may be as high as 0.7 wt% depending on the melt composition, pressure, and temperature. It increases with T, P and the polymerization state of the liquid. Characterization by Raman spectroscopy and ^{15}N solid state MAS NMR indicates that nitrogen is not only physically dissolved as N_2 within the melt structure like noble gases, but a fraction of nitrogen interacts strongly with the silicate network. The most likely nitrogen-bearing species that can account for Raman and NMR results is nitrosyl group. Solubility data follow an apparent Henry's law behavior and are in good agreement with previous studies when the nitrosyl content is low. On the other hand, a significant departure from a Henry's law behavior is observed for highly depolymerized melts, which contain more nitrosyl than polymerized melts. Possible solubility mechanisms are also discussed. Finally, a multi-variant empirical relation is given to predict the relative content of nitrosyl and molecular nitrogen as a function of P, T, and melt composition and structure. This complex speciation of nitrogen in melts under high pressure may have significant implication concerning crystal–melt partitioning of nitrogen as well as for potential elemental and isotopic fractionation of nitrogen in the deep Earth.

1. Introduction

Nitrogen is the major volatile element of the Earth's atmosphere. It is therefore critical to determine its physical properties and its chemical reactivity with geomaterials to understand and quantify processes that may have controlled its exchange between the solid Earth and the atmosphere. Indeed, nitrogen, like noble gases, is a prime geochemical and cosmochemical tool to unravel differentiation processes which took place after the accretion of Earth-like bodies, and lead to the formation of a layered solid Earth, a hydrosphere and an atmosphere (e.g., Javoy, 1997; Tolstikhin and Marty, 1998; Marty and Dauphas, 2003). In this respect, extraction of volatiles from a hypothetical magma ocean or from the solid Earth through partial melting and degassing of mantle-derived magmas played a central role.

Mechanisms governing the incorporation of nitrogen in silicate melts are not extensively documented. Because N_2 has one of a strong covalent bond, its behavior is generally assumed to resemble that of noble gases. The latter have been widely studied in the past decades (Kirsten, 1968; Hiyagon and Ozima, 1986; Jambon et al., 1986; Lux, 1986; Carroll and Stolper, 1991, 1993; Broadhurst et al., 1992; Miyazaki et al., 1995, 2004; Chamorro-Perez et al., 1996, 1998; Shibata et al., 1998; Schmidt and Keppler, 2002; Brooker et al., 2003). At relatively low pressure, the solubility of these inert gases is relatively low, thus allowing an efficient degassing of magmas. Their partitioning between crystal–melt and melt–vapor phases follow Henry's laws at low pressure and are essentially incompatible elements. Finally, their solubilities in melts decrease significantly with the increase of their atomic radius, a behavior

* Corresponding author. Fax: +1 202 478 8901.
E-mail address: m.roskosz@gl.ciw.edu (M. Roskosz).

0016-7037/$ - see front matter © 2006 Elsevier Inc. All rights reserved.
doi:10.1016/j.gca.2006.03.001

consistent with a steric effect: these gases fill empty spaces within the melt network.

At near ambient pressure and under oxidizing conditions, nitrogen qualitatively follows similar patterns (Doremus, 1966; Marty, 1995; Miyazaki et al., 1995; Libourel et al., 2003). However, its behavior is quite different under reducing conditions (Mulfinger, 1966; Libourel et al., 2003; Miyazaki et al., 2004). For instance, other parameters being equal, nitrogen contents typically vary by 5 orders of magnitude as a function of the redox conditions within a MORB-like liquid (Libourel et al., 2003). This effect is due to a change of the solubility mechanism. Under oxidizing conditions and at low pressure, nitrogen is dissolved as N_2 within the empty spaces of the silicate network and do not interact with it. Conversely, under reducing conditions nitrogen is chemically bound to the silicate (Mulfinger, 1966). Extremely reducing conditions are required, though, to reach these conditions at ambient pressure. Typically, nitrogen does not interact with the silicate for oxygen fugacity (fO_2) above $10^{-10.7}$, corresponding to an fO_2 one order of magnitude below the iron-wüstite buffer (IW) at 1400 °C. Because the redox state of the mantle is unlikely to be below IW since the Archean (e.g., Canil, 2002), nitrogen behavior is thus expected to be really comparable to that of noble gases at ambient pressure (Marty, 1995; Libourel et al., 2003).

At high pressure however, the behavior of volatiles is less well understood and more complicated. For instance, concerning noble gas, available data show that the solubility is very sensitive to the chemical composition of the silicate melt (Chamorro-Perez et al., 1996, 1998; Shibata et al., 1998; Schmidt and Keppler, 2002; Brooker et al., 2003; Bouhifd and Jephcoat, 2006). Their solubility may decrease above a few GPa or just become pressure-independent. As a consequence, the partitioning of noble gases between melts and minerals may change with pressure so that these elements becoming progressively moderately incompatible to compatible. The only general agreement is that at high pressure, the Henry's law breaks down (Sarda and Guillot, 2005). In addition, the first evidence for a xenon silicate has recently been found at ultra-high pressure (Sanloup et al., 2002). By analogy, the behavior of nitrogen may also be more complicated at high pressure. Furthermore, a dramatic enhancement of the reactivity of N_2 at high pressure has actually been confirmed recently. Indeed, previously unknown nitrides such as platinum nitride (PtN) may be prepared by compressing Pt above 45 GPa in a diamond anvil cell and using N_2 as a pressure medium (Gregoryanz et al., 2004).

Understanding how nitrogen and other volatiles progressively lose their inert behavior is crucial because if it occurs at different pressures, then a significant fractionation among these species may occur and the composition of the different reservoirs may be misestimated by the records of atmospheric, basaltic and xenolith samples. Thus, high-pressure data on solubility and solubility mechanisms are required to constrain better the budget of volatiles of the different geochemical reservoirs.

No studies have been dedicated to the solubility and, more importantly, to the speciation of nitrogen in silicate melts at kilobars total pressures. For this purpose we have investigated both the solubility and the speciation of nitrogen in nominally anhydrous alkali-, and alkaline-earth silicate melts at pressures ranging from 10 to 30 kbar and temperature ranging from 1400 to 1700 °C. Raman spectroscopy and ^{15}N solid state MAS NMR were employed to study the speciation of nitrogen under these conditions. It is found that a significant fraction, and sometime a dominant fraction of this volatile interacts strongly with the silicate melt despite a moderately oxidized state.

2. Experimental methods

2.1. Starting compositions

Nine glasses were synthesized: three sodium silicates [Na_2O–$2SiO_2$ (NS2), Na_2O–$4SiO_2$ (NS4), Na_2O–$8SiO_2$ (NS8)], a potassium [K_2O–$4SiO_2$ (KS4)] and a lithium silicate [Li_2O–$4SiO_2$ (LS4)], a calcium, a strontium, and a barium silicate [CaO–SiO_2 (CS), SrO–SiO_2 (SrS), BaO–SiO_2 (BaS), respectively], and finally an anorthite–diopside eutectic glass (CMAS). Nominal compositions of these starting materials are given in Table 1. The use of sodium silicates is justified by their low melting points, their moderately hygroscopic behavior compared to other alumina-free glasses and the wide range of composition over which homogeneous glass can be prepared (without liquid–liquid immiscibility). These three sodium silicates cover up a large range of polymerization state and, thus, provide a measure of the effect of this structural parameter on the solubility behavior of nitrogen. Potassium and lithium silicates were selected to compare the effect of the alkali cation on the nitrogen solubility behavior, other parameter being equal. A ratio M_2O/SiO_2 of 1:4 was selected because at higher potassium content, the glass is too hygroscopic to be considered as anhydrous at virtually any condition. Conversely, at lower Li content, subliquidus liquid–liquid metastable phase separation occurred very fast, even during the quench. Though ultramafic melts are obviously the target of such a study of silicate melts at high pressure, they cannot be directly studied because of experimental

Table 1
Nominal compositions of starting glasses (in mol%)

	NS2	NS4	NS8	KS4	LS4	SrS	CMAS
SiO_2	66.66	80	89.99	80	80	50	53.55
Al_2O_3							9.8
MgO							11.01
CaO							25.64
SrO						50	
Na_2O	33.33	20	11.11				
K_2O				20			
Li_2O					20		

limitations. As a consequence, the effect of alkaline-earth cations has been studied through simple binary melts with a polymerization state ressembling ultramafic melts. Such melts may be prepared and studied at high pressure (CS, SrS, BaS). Even within this restricted range of composition, only the strontium silicate was found to be quenchable to a glass from high temperature, high pressure experiments. In spite of the structural complexity of CMAS glasses, which prevent any simple quantification of the interaction between nitrogen and such melts, an anorthite–diopside eutectic was studied because it is often considered as a good, synthetic analog of the 'Silicate Earth'.

All these glasses were synthesized from mixtures of reagent grade SiO_2, Al_2O_3, Na_2CO_3, K_2CO_3, Li_2CO_3, $CaCO_3$, $MgCO_3$, $SrCO_3$, $BaCO_3$, first fired at relevant temperatures to dehydrate them (between 300 and 1000 °C). Samples were melted in air in thin-walled Pt crucible at temperature between 1000 and 1600 °C. These temperatures depend on the melting point of compositions and were optimized in order to prevent significant alkali volatilization during the process.

2.2. The solid-state nitrogen source employed

The fraction of nitrogen dissolved in these melts, especially at high pressure, is expected to be relatively large. As a consequence, the use of a solid source of nitrogen was required to ensure that complete saturation of the liquid was achieved. Generally, the nitrogen source used in high-pressure experiments are guanidine nitrate or ammonium, used in the presence of oxygen buffers (Holloway and Reese, 1974). Heating several other nitrates may also lead to generate an N_2–O_2 atmosphere. In the latter case, the vapor composition accessible by these methods is restricted and determination of the speciation of nitrogen is not trivial. Furthermore, the use of these components generally implies a contamination of the melt by non-volatile by-products resulting from the thermal decomposition of the nitrogen-bearing molecules.

The only way to obtain a nominally pure N_2-atmosphere is to use an azide (Keppler, 1989). We used a silver azide (AgN_3), an extremely unstable and explosive compound. It was synthesized by mixing solutions of reagent grade silver nitride ($AgNO_3$) and sodium azide (NaN_3) following the protocol described by Keppler (1989). Because this product is very unstable, it was not dried but used in the form of a suspension in distilled water, and was stored in an opaque Teflon container because it is slowly decomposed by light. A small amount of ^{15}N-labeled silver azide was also prepared for NMR experiments (33% of ^{15}N). For this purpose, isotopically labeled sodium azide (Cambridge Isotope Laboratories, Inc.) was employed to prepare the AgN_3.

With this nitrogen compound, a nominally pure N_2-atmosphere is produced even at temperature below 350 °C because AgN_3 is thermodynamically unstable with respect to silver and nitrogen at all P–T conditions of interest. Thus, even before the melting of silicate glasses, AgN_3 breaks down to Ag^0 and N_2. Another advantage of this method is that Ag^0 readily makes an alloy with the platinum used to prepare capsules. In other words, the use of this compound does not lead to any contamination of the starting silicate as confirmed by electron microprobe analyses. However, in presence of other redox couples like Fe^0/Fe^{2+}, or Fe^{2+}/Fe^{3+}, a redox reaction occurs with Ag^0. Metallic silver is oxidized to Ag^+ and is stabilized in melts. This is why iron-bearing melts have not yet been studied. Additional problems attached to the study of iron-bearing liquids includes the following: (1) part of iron is always lost in Pt capsules, (2) Fe precludes the use of NMR, and (3) significant fluorescence decreases the signal/noise of Raman spectra considerably particularly in the high frequency region, where nitrogen Raman bands are expected.

2.3. Run procedure

Experiments were performed with a solid-media, Boyd–England piston–cylinder press (Boyd and England, 1960) and using sealed platinum capsules. Silver azide was added as a suspension in such a way that a quantity of 2 mg of dry azide was obtained. The capsule was then dehydrated at 105 °C, a temperature at which the decomposition of the azide is very sluggish and not explosive. We left the sample at this temperature until no mass changes could be measured using a high precision Mettler AE 240 microbalance. Typically 6 h was required to reach this plateau, but we left the capsule at 105 °C for 12 h. Then, about 10 mg of glass powder was added. The capsule was then welded in air or in ultrapure argon flow, while the bottom was cooled in water to prevent any blow-out during this stage.

Capsules were then placed in 3/4″ or 1/2″ talc–Pyrex sleeves assemblies. Graphite heaters were employed and samples were packed in previously dehydrated MgO powder. Temperature was controlled by a $Pt–Pt_{10}Rh$ thermocouple. The pressure uncertainty is ±1 kbar. Samples were heat-treated over a temperature range between 1400 and 1700 °C and a pressure range between 10 and 30 kbar (Table 2). The 3/4″ assemblies were used to allow the heating of three different samples at exactly the same conditions. On the other hand, 1/2″ assemblies were used to allow a faster quench. No significant differences were observed among samples prepared in both techniques, either in terms of nitrogen content or in terms of the Raman spectra of the glasses.

Typical run duration was 60 min though shorter and longer runs have been performed to determine more accurately the time required to reach the equilibrium (see below). After an experiment, capsules were cleaned and opened. Samples are generally crystal-free, translucent yellowish glasses. When this was not the case, samples were discarded with the exception of strontium silicate for which only partly crystallized samples could be recovered and analyzed. Some bubbles are present but they are randomly distributed. This suggests a saturation of the sample in

Table 2
Experimental conditions

Composition	Pressure (kbar)	Temperature (°C)	Type of assembly	Run duration (min)
NS8–blank	15	1650	3/4″	60
NS4–blank	15	1650	3/4″	60
NS2–blank	15	1650	3/4″	60
NS2–Ar	20	1400	1/2″	60
NS2–Ar	20	1600	1/2″	60
NS2–^{15}N	20	1600	3/4″	180
NS2	20	1600	1/2″	90
NS2	20	1600	1/2″	40
NS2	20	1600	1/2″	20
NS8	10	1600	3/4″	60
NS4	10	1600	3/4″	60
NS2	10	1600	3/4″	60
NS8	15	1650	3/4″	60
NS4	15	1650	3/4″	60
NS2	15	1650	3/4″	60
NS8	20	1700	3/4″	60
NS4	20	1700	3/4″	60
NS2	20	1700	3/4″	60
NS2	20	1400	1/2″	60
NS2	20	1500	1/2″	60
NS2	20	1600	1/2″	60
NS2	10	1600	3/4″	60
NS4	20	1600	3/4″	60
NS4	10	1600	3/4″	60
NS2	10	1600	3/4″	60
NS2	30	1600	1/2″	60
LS4	17	1600	3/4″	60
NS4	17	1600	3/4″	60
KS4	17	1600	3/4″	60
SrS	10	1700	3/4″	60
CMAS	20	1600	1/2″	60

volatiles rather than a partial degassing during the quench (Fig. 1), which is characterized by heterogeneously distributed and locally concentrated bubbles conferring a cloudy appearance to the sample. Half of the glass chips were then mounted as polished sections for electron microprobe analysis and other chips were directly analyzed with the Raman spectrometer to prevent any dissolution of atmospheric water after the experiment.

2.4. Raman spectroscopy

Raman spectra were recorded in a backscattering geometry with a XY DILOR Raman microspectrometer equipped with a CCD detector. The 514.5 nm line of a Spectra Physics Ar^+ laser was focused on the sample down to a 2 μm spot through a microscope objective (50×) that was also used to collect the backscattered Raman light.

At least five different glass chips of the same samples were analyzed. A linear base line was fitted to the high frequency region (especially around the region of nitrogen stretching modes) of all the spectra and a temperature–frequency correction of the Raman intensity was applied (Long, 1977). A more unusual procedure was then employed because of the presence of atmospheric nitrogen into the spectrometer itself: a Raman spectrum of nitrogen from the ambient is observed when no sample is illuminated. To remove this ''blank'' signal, a Raman spectrum of the air was recorded with the same analytical conditions as the samples. This procedure was followed at the beginning of each analytical session. In this way, after the base line and the temperature–frequency correction, this signal was removed from the spectra. Once this correction applied, spectra were compared directly. Spectra of glasses with different composition were compared without intensity normalization because no normalization is rigorously valid in this case since these glasses have very different distribution of Q-species (Maekawa et al., 1991). However, when samples of the same composition were compared, all the spectra were normalized to the most intense peak of the silicate region.

2.5. ^{15}N solid state magic angle spinning nuclear magnetic resonance spectroscopy

^{15}N solid state MAS NMR spectra were acquired using single pulse methods, employing a 4.5 μs excitation pulse, a spectral width of 40 kHz, an acquisition time of 25 ms, and a sample spinning speed of 10 kHz. The magnetic field is 7.05 T; the larmor frequency of ^{15}N at this field strength

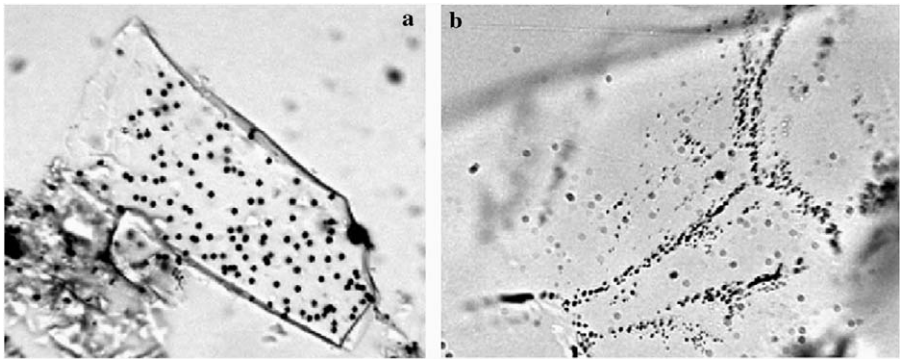

Fig. 1. Optical micrographs of samples quenched from high pressure and temperature (same scale, magnification 20×). (a) Large bubbles randomly distributed within a NS2 glass chips, indicating a saturation of the liquid in volatile. (b) Small bubbles concentrated along preferential path in a NS2 glass chips, indicating a partial exsolution of the volatile phase during the quench. Such samples were discarded.

is ~30 MHz. We note that a 90° pulse requires a recycle delay greater than 5 × T1. Given the very weak signal associated with low abundance of N in these glasses no attempt was made to measure T1, but we have measured the T1 of ^{29}Si with Gadolinum oxide added as a relaxation agent and measured a T1 of less than 20 ms. We assume, therefore, that 1 s recycle delay is sufficient to avoid longitudinal saturation. Due to the relatively weak signal resulting from the low abundance of nitrogen in these samples, 640,000 acquisitions were obtained per sample. The time domain signal was zero-filled to 8192 points and line broadening of 200 Hz was applied prior to Fourier Transformation. Spectra were referenced to the ^{15}N resonance of solid glycine (defined as 10 ppm relative to ammonium chloride solution = 0 ppm).

2.6. Chemical analyses

Samples were polished dry and only ethanol was used to clean them in order to minimize their hydration. Chemical analyses were made with a JEOL 8800 operating at 10 nA, 15 kV. The standardization was done using a synthetic basalt glass. Boron nitride was used as a standard for nitrogen. It is of note that microprobe is not the most efficient apparatus to analyze nitrogen compared to UVLAMP (e.g., Brooker et al., 1998) or ion probe techniques (e.g., Hashizume et al., 2000), but this simple technique has been found reliable and reproducible given the high nitrogen content of our glasses. The reported nitrogen contents represent an average of more than 10 analyses in the areas with no bubbles that would distort the chemical analysis. Repeated analyses on the same area showed no difference of the nitrogen content.

Only sodium silicates were analyzed. The KS4 samples were not analyzed because the preparation and storage of this hygroscopic glass for microprobe analyses may have altered the nitrogen content. Finally, the detection of lithium did not allow the determination of any reliable composition. In the case of sodium-bearing silicates a large area (~100 μm^2) was analyzed to minimize this volatilization. Volatilization was negligible for NS8 and NS4 glasses and very low for NS2. Analyses performed on NS8 with different acquisition times do not lead to any change of the determined nitrogen content. A loss associated with sodium volatilization in the case of NS2 cannot be ruled out though. It must however be restricted to an acceptable level given the fact that no correlation could be found between the nitrogen content measured and the fraction of sodium lost under the electron beam.

3. Results

3.1. Nitrogen content of glasses quenched from high-pressure and high temperature

The nitrogen content of NS8, NS4, and NS2 glasses temperature-quenched at high pressure ranges from 0.3 to 0.7 wt% with typical uncertainties of the order of 0.03 wt%. It is systematically higher for NS8 than for NS2. This is particularly obvious at the highest P and T conditions (Fig. 2a). The increase of temperature results in an increase of the nitrogen content. The temperature dependence is higher for NS2 than for NS4. For instance, in the former case, X_{N_2} increases by almost a factor of two over 300 °C (Fig. 2b). The temperature dependence is linear within the analytical error. The pressure has qualitatively the same effect as temperature but its effect is more pronounced for polymerized melts (Fig. 2c).

3.2. Spectroscopic evidence for a dual behavior of nitrogen dissolved in silicate melts

At ambient pressure, the main vibron of the N_2 molecule is located at 2331 cm^{-1}. Therefore, our study focuses mainly on the high frequency region of the spectrum (2000–2500 cm^{-1}). This region shows some significant variations as a function of experimental conditions. In glasses prepared at ambient pressure in air, only the aforementioned lorentzian band near 2331 cm^{-1} is observed. It likely embodies the air trapped in the spectrometer, rather than the nitrogen dissolved in glasses as explained above. Nominally nitrogen-free melts quenched from high pressure but still synthesized with air trapped in the sealed container are not different (Figs. 3 and 4). Only the structure of the silicate network is modified. These differences in the low frequency envelope illustrate changes of the relative contents of Q-species within the melt at increasing pressure, as repeatedly described for such compositions (Dickinson et al., 1990; Mysen, 1990; Xue et al., 1989).

This picture is different when nitrogen is added. First, the typical vibron of N_2 is no longer a sharp, lorentzian peak but becomes broader and Gaussian (Fig. 4). This broadening is interpreted as the result of the distortion of N_2 molecules trapped in interstitial sites within the silicate structure. The dependence of this distortion as a function of intensive and compositional parameters is addressed below. More importantly, two additional and even broader bands are resolved at lower frequencies, around 2100 and 2200 cm^{-1} (Fig. 4). These additional bands are rather independent of the initial composition of the gas mixture trapped in the platinum capsule. Indeed, samples prepared in air or under a flow of argon (ultra high purity) do not show significant differences in terms of signal intensity or frequency (Fig. 4). In these samples, no significant amount of dissolved water was detected by Raman spectroscopy.

^{15}N-labeled AgN_3 was used to characterize further the speciation of nitrogen in these melts. As detailed below, the intensity of the Raman bands in addition to that near 2331 cm^{-1} are higher for NS2 than for other sodium silicate glasses. This glass was, therefore, the main composition examined with ^{15}N NMR and Raman spectroscopy. Raman spectra of samples prepared with labeled nitrogen

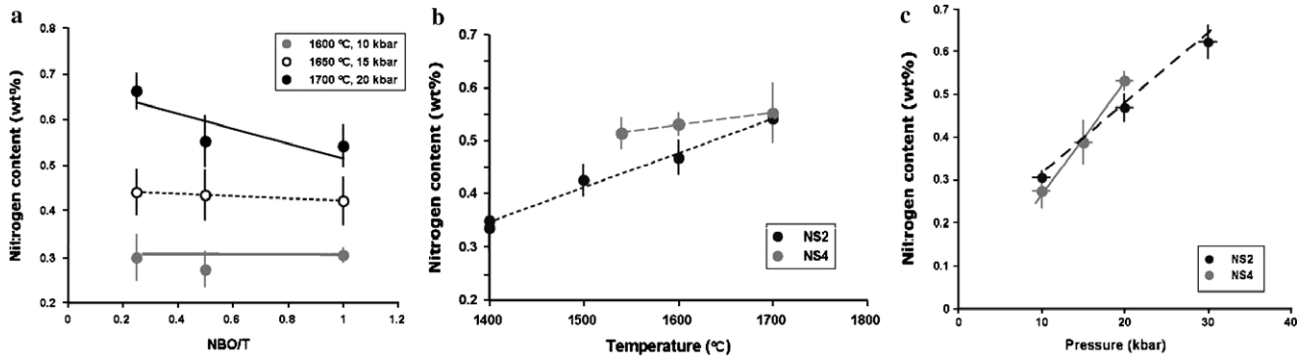

Fig. 2. Nitrogen content of glasses quenched from high pressure and temperature: (a) as a function of NBO/T, (b) as a function of temperature for NS2 and NS4 glasses synthesized at 20 kbar, (c) as a function of pressure for NS2 and NS4 glasses synthesized at 1600 °C. Lines are only guides for the eyes.

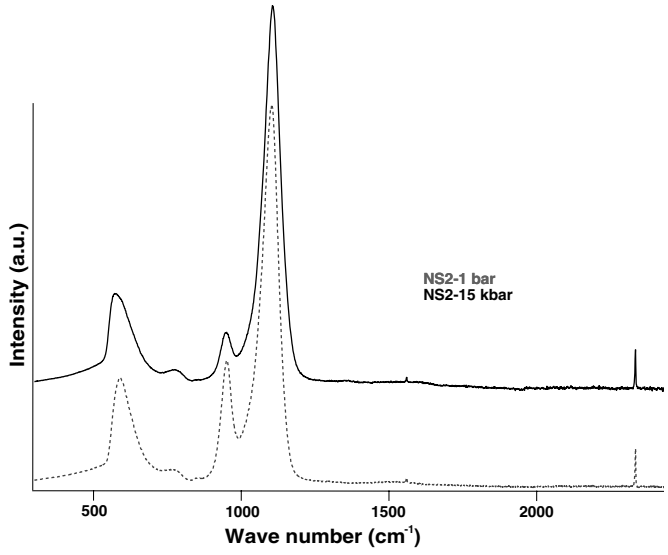

Fig. 3. Typical Raman spectra of nominally nitrogen-free NS2 glasses prepared at ambient pressure and at 15 kbar. Relative intensities of bands forming the broad envelope around 1000 cm^{-1} are pressure dependent and are assigned to the distribution of the Q-species in the glass. Besides, no significant changes are observed especially above 2000 cm^{-1} where only the signal of atmospheric nitrogen is observed.

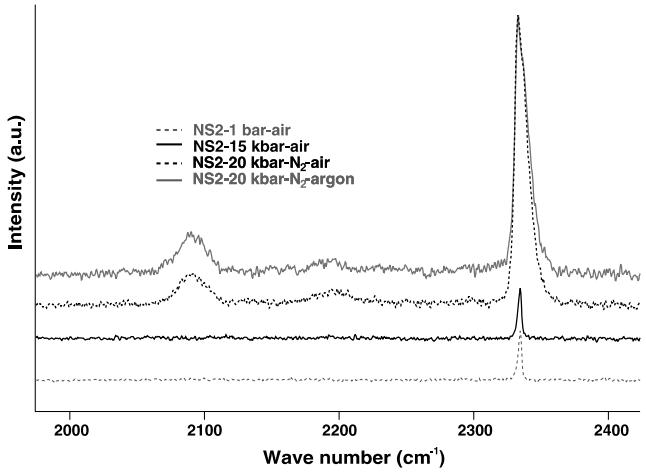

Fig. 4. High frequency region of typical Raman spectra of glasses prepared in different experimental conditions. Without addition of nitrogen into the capsule, the only Raman signal collected is that of the atmospheric nitrogen. When azide is poured into the capsule, this vibron has a higher intensity and additional bands are observed. The presence of air or pure argon into the capsule before the run does not affect significantly the Raman spectra of the samples. In this figure, Raman spectra are not corrected for atmospheric nitrogen.

revealed a strong isotopic effect (Fig. 5). For instance, the single vibron of N_2 is split in three bands with very different frequencies. Such isotopic effect on the vibration frequency of this diatomic molecule can be predicted using the Hooke's law for a harmonic oscillator

$$\bar{\nu} = \frac{1}{2\pi c}\sqrt{\frac{k}{\mu}}, \tag{1}$$

where $\bar{\nu}$ is the frequency, c is the light velocity, k is the force constant and μ is the reduced mass defined as

$$\mu = \frac{m1 \cdot m2}{m1 + m2}, \tag{2}$$

where $m1$ and $m2$ are the masses of the atoms. Because the frequency of the vibron for $^{14}N{\equiv}N^{14}$ is well known, the frequency of $^{15}N{\equiv}N^{14}$ and $^{15}N{\equiv}N^{15}$ can be easily derived using Eq. (1). As shown in Fig. 5 and Table 3, the three

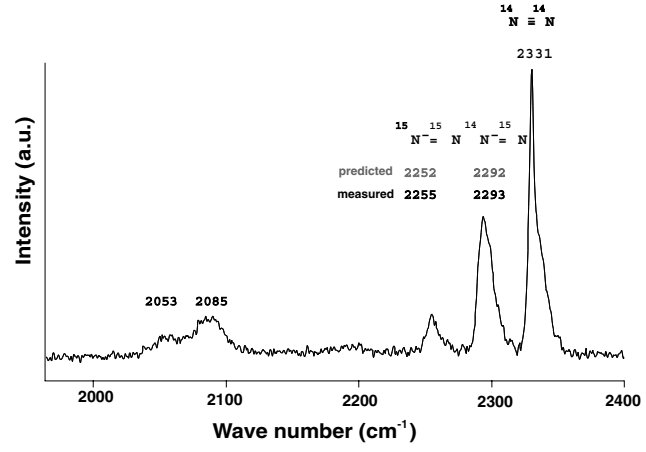

Fig. 5. High frequency region of the Raman spectra of a NS2 glass quenched from HT-HP and containing ^{15}N-labeled nitrogen. The isotopic substitution induces the split of the Raman signature of nitrogen-bearing groups. This shift is used to infer the nature of these groups (see text and Table 3). In this figure, Raman spectra are not corrected for atmospheric nitrogen.

high-frequency bands are characteristic of molecular N_2 with different isotopic compositions.

The lower-frequency band, between 2100 and 2200 cm^{-1} (Fig. 4) is also affected by the isotopic substitution. This confirms first that this signal refers directly to a nitrogen-bearing molecule and cannot be attributed to any indirect modification of the silicate network during experiments. Moreover, it is likely that only a single N atom is involved because the Raman band is split in two. If two N atoms were involved, the band would be split in three. The frequency shift induced by the isotopic substitution can be estimated assuming different kind of diatomic oscillator (e.g., NSi, NO, NH). Only NO– molecules containing ^{14}N and ^{15}N can account for the frequency shift measured experimentally, whereas a substitution ^{14}N–^{15}N in NSi and NH groups leads to a too large and to small frequency shift, respectively (Table 3). This result thus suggests interactions between nitrogen and oxygen of the silicate network at high temperature and high pressure. There is a plethora of studies dedicated to the structure of nitride glasses (e.g., Rouxel et al., 1990; Grande et al., 1995; Sakka, 1995; Rouxel and Piriou, 1996; McMillan et al., 1998; Navarro, 1998). Raman bands in the frequency region 2000–2200 cm^{-1} have never been reported for such glasses, supporting the fact that Raman bands observed cannot be assigned to any NSi group. Based on Raman spectroscopy, nitrosyl group is the most likely candidate.

^{15}N solid state MAS NMR experiments have been carried out on the same sample. This spectroscopy provides a relatively wide spectral window for separating nitrogen species based on oxidation state as it affects nuclear shielding. Reduced nitrogen experiences the greatest shielding, hence ammonia and amines resonate in the lowest frequency range of the ^{15}N spectral region. If we refer the ^{15}N spectrum to the resonant frequency of ammonium chloride, defining this resonance as lying at 0, then we note that the ^{15}N spectrum extends up to near 400 ppm where the ^{15}N resonance of highly deshielded nitrate is observed. Virtually all other ^{15}N species lie between 0 and 400 ppm.

Table 3
Calculated Raman frequency shift induced by the substitution of ^{14}N by ^{15}N in an harmonic diatomic oscillator

Diatomic molecule	Frequency calculated (cm^{-1})	Frequency observed (cm^{-1})
^{14}N–^{14}N	2331	2331[a]
^{14}N–^{15}N	2291	2293
^{15}N–^{15}N	2251	2255
^{14}N–O		2085[a]
^{15}N–O	2049	2053
^{14}N–Si		2085[a]
^{15}N–Si	2038	2053
^{14}N–H		2085[a]
^{15}N–H	2081	2053

[a] Raman frequency shifts are calculated for isotopically substituted molecules assuming that this band may be assigned to the stretching of its non-substituted counterpart (see the main text).

In Fig. 6, the ^{15}N solid state spectrum of the NS2 glass is presented. Two nitrogen-bearing species are clearly observed with peaks at 289 and 253 ppm (relative to NH_4Cl); A pair of nitrogen-bearing species is consistent with what is detected via Raman spectroscopy (Figs. 4 and 5). The larger 289 ppm peak (~85% of the total resonance intensity) most likely corresponds to N_2 located within the NS2 glass matrix. This frequency is consistent with triply bonded nitrogen, e.g., "CN" groups resonate in the 200–230 ppm range, substitution of nitrogen for carbon would reasonably decrease the shielding leading to a slightly higher frequency resonance of N_2. This frequency is also consistent with that of N_2 gases measured by Jameson et al. (1981). The nitrogen species responsible for the smaller peak at 253 ppm (15% of the total intensity) cannot be identified directly from these data but the following conclusions can be made. First, the relatively high frequency unambiguously excludes the possibility that this peak indicates the presence of ammonium cations. Second, in the discussion above, the Raman data indicate the presence of a second N-bearing species, possibly NO or bound nitrosyl groups. Given that the triple bond will have the most significant affect on the shielding characteristics of nitrogen, the presence of this smaller peak near N_2 and "CN" is consistent with triply bonded nitrogen; plausibly NO or nitrosyl. Based on the combination of NMR and Raman data, it is thus proposed that the intense peak around 2100 cm^{-1} embodies nitrosyl groups present in the silicate network. It is not possible to assign the third and least intense peak (2200 cm^{-1}) detected by Raman spectroscopy. The crude correlation between the area under this peak and the one at 2100 cm^{-1} indicates that both are probably related to the same nitrogen-bearing group. However the intensity of this peak is too weak to resolve this environment by

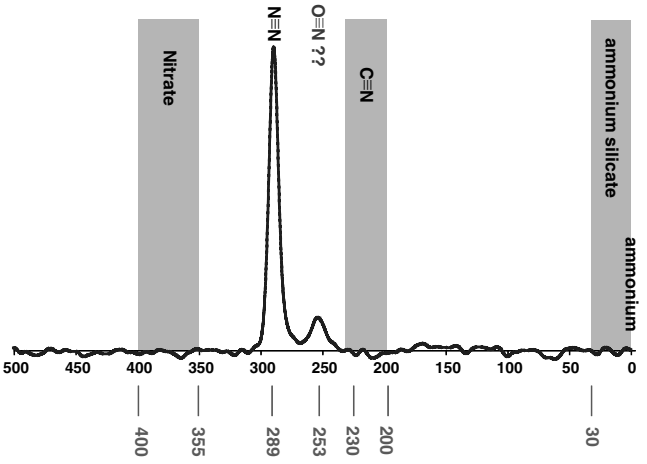

Fig. 6. ^{15}N solid state NMR spectrum of a nitrogen-bearing glass, NS2, acquired with single pulse excitation and 10 kHz magic angle sample spinning. Two nitrogen-bearing species are clearly evident in this glass. The spectral ranges corresponding to reduced nitrogen, e.g., ammonium and amines (~0–30 ppm); triply bonded cyano ("CN") nitrogen (~200–230 ppm); and oxidized nitrogen, e.g., nitrate (~335–400 ppm). The larger peak at 289 ppm is most likely N_2; the smaller peak at 253 ppm may correspond to NO (??).

NMR spectroscopy. It is thus impossible to know if the two peaks represent simply different local environments of NO– groups.

3.3. A contrasted time-, composition-, temperature-, and pressure-dependence of the Raman scattering of dissolved nitrogen in silicate melts

3.3.1. Time-dependence and gas–liquid equilibration

Time series were performed with the NS2 composition. Samples prepared in comparable conditions of pressure and temperature were quenched after 20, 40, and 90 min in order to document the kinetics of nitrogen dissolution in melts. Because of the experimental setup and in particular because the starting glass is finely crushed, the gaseous nitrogen embedded glass chips (grain size typically <100 μm) before the melting. Therefore, it was expected that the dissolution occurred rapidly. At ambient pressure, it has been observed that a minimum of 10 h was required to equilibrate a liquid with the gas phase (Libourel et al., 2003). In this case, however, diffusion of N_2 had to proceed through Pt or graphite crucible containing 300–500 mg of liquid. Our results indicate that the Raman signature of nitrogen dissolved in glasses does not change after 40 min (Fig. 7). The intensity of molecular nitrogen (~2300 cm^{-1}) does not change significantly between 20 and 90 min. Furthermore, typical high-pressure experiments dealing with gas–melt equilibration are performed for 1–2 h (e.g., Schmidt and Keppler, 2002). This result suggests that under these pressure and temperature conditions, the diffusion of nitrogen trapped between glass chips is fast and equilibration occurs within a few tens of minutes. On the other hand, intensities of other peaks (~2100 and ~2200 cm^{-1}) change over time. The signal increases by a factor of 2 between 20 and 40 min. For longer run duration, no further increase of these intensities can be noted. Chemical reactions that lead part of N_2 to interact with the silicate network are thus slower than the pure diffusion of the gas into the melt but the steady state is reached after 40 min. To ensure a complete equilibration, we have set the time duration of other experiments to 60 min.

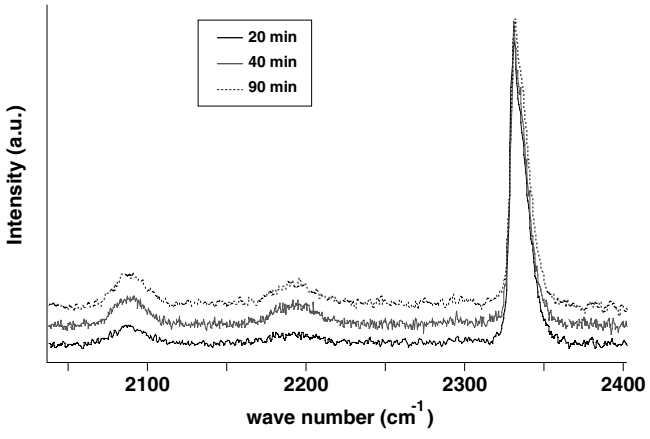

Fig. 7. Effect of the run duration on the high frequency region of the Raman spectra of NS2 glasses prepared at 1600 °C and 20 kbar. A steady state is reached at 40 min. In this figure, Raman spectra are not corrected for atmospheric nitrogen.

3.3.2. Influence of the gas mixture composition and of the nitrogen partial pressure

The control of the volatiles partial pressures is a major concern during high pressure, high temperature experiments. It was virtually impossible to buffer precisely gas fugacities. However, the hypothetical influence of the gas mixture on the Raman spectra may provide an insight into this issue. First of all, we note that the presence of air or pure argon in the capsule does not change any feature either qualitatively or quantitatively (Fig. 4). Besides, Libourel et al. (2003) and Miyazaki et al. (2004) demonstrated that the composition of the gas mixture did not affect nitrogen solubility unless conditions are strongly reducing (below IW-1). In this latter case, the composition of the gas phase has a critical effect on the nitrogen solubility because silicone nitride is produced. Such complex was never observed in any of our experimental charges and is not consistent with the redox state of nitrogen inferred by NMR results. We thus conclude that experiments took place under oxidizing to moderately reducing conditions.

The amount of nitrogen produced by the decomposition of AgN_3 exceeds the amount of nitrogen that could readily be dissolved into the melt. The drawback of this design is that the extrapolation of such results to realistic nitrogen content such as those currently measured in natural magmas is not straightforward. We carried out experiments with various amounts of AgN_3 between 0.8 and 4.6 mg. No obvious and systematic changes were observed in Raman spectra of the different samples. Especially, the relative intensities of the bands do not change. It is worth noting that these experiments are all N_2 oversaturated but we think it may be reasonably assumed that results described below are valid even under low nitrogen partial pressure (i.e., experimental conditions which would prevent the study of the nitrogen speciation in melts).

3.3.3. Effect of the melt polymerization state

A critical parameter that controls many properties of magmas is their polymerization state. This parameter is generally quantified by the number of non-bridging oxygen per tetrahedrally coordinated cation (NBO/T). Glasses NS2, NS4, and NS8 have been selected to cover a wide range of NBO/T, respectively: 1, 0.5, and 0.25. For these three compositions, the speciation of nitrogen has been studied at different pressures and temperatures. For given pressure and temperature, three samples (one of each composition) were heat-treated together to insure strictly identical experimental conditions. Raman spectra were recorded during the same session and in the same conditions for a given experimental run. In this way, spectra can be compared directly.

The dual speciation of nitrogen is obvious regardless of pressure, temperature and polymerization state (Figs. 8a,b, and c). However, the intensity of the peak at 2200 cm^{-1} is very low to negligible for NS4 and NS8, whereas intensities of peaks at 2100 and 2300 cm^{-1} are always significant. A consistent picture emerges that is independent of pressure and temperatures: the intensity of the peak at 2300 cm^{-1} is higher for the most polymerized, silica-rich melts, whereas the intensity of the peak at 2100 cm^{-1} is higher for depolymerized, silica-poor melts. In addition, the shape of the peak at 2300 cm^{-1} changes with composition and shifts toward higher frequency and is broader for depolymerized melts than for polymerized ones. This result is consistent with the dissolution of molecular nitrogen in interstitial position within the melt structure. The decrease of the signal intensity with the increase of the melt depolymerization is thus related to the more compact structure of these glasses. This structural interpretation also accounts for the increase of the distortion of N_2 molecules as indicated by the line broadening and the frequency shift (Fig. 8b).

The Raman cross section of the different Raman bands is unknown and as a consequence it is difficult to quantify the relative amount of these species. However, we have rationalized spectroscopic data by calculating the ratio of the area below peaks at 2100 cm^{-1} over peaks at 2300 cm^{-1}. It is not possible to derive accurate error bars for these ratios but typically the accuracy cannot be better than 5%. Whatever the real accuracy is, this method allows comparison of the spectra of data for all the samples (any P, T, X).

The intensity ratio of the 2100 to 2300 cm^{-1} bands does not change significantly for NS8 and NS4, and decrease significantly with increasing P and T for NS2 (Fig. 8d). The non-linear relation between this ratio and the polymerization state prevailing at low pressure and temperature becomes linear at high pressure and temperature.

3.3.4. Temperature dependence

All other parameters being equal, an increase of temperature results in an increase of the intensity of the peak at 2100 cm^{-1} and a decrease of the peak assigned to vibrations in molecular nitrogen. The intensity of the peak at 2200 cm^{-1} does not change significantly (Figs. 9a and b). This feature is obvious for NS2 glasses because the temperature range studied is large but the same trend is also observed for NS4 glasses. No significant frequency shift or any change in the peak shape occurs with the increase of temperature. This observation indicates that temperature has no effect on the distortion of nitrogen-bearing species or that this effect is not recorded in quenched glasses. The area measured below the peaks of molecular N_2 is a linear function of the temperature (Figs. 9c and d). Conversely, the increase of the area below the peak at 2100 cm^{-1} may be a non-linear function of temperature.

3.3.5. Pressure dependence

The intensity of the signal of N_2 (2300 cm^{-1}) increases with total pressure. There is a significant frequency shift toward higher wave number and a significant broadening of the Raman signal of N_2 (Figs. 10 a and b). This broadening

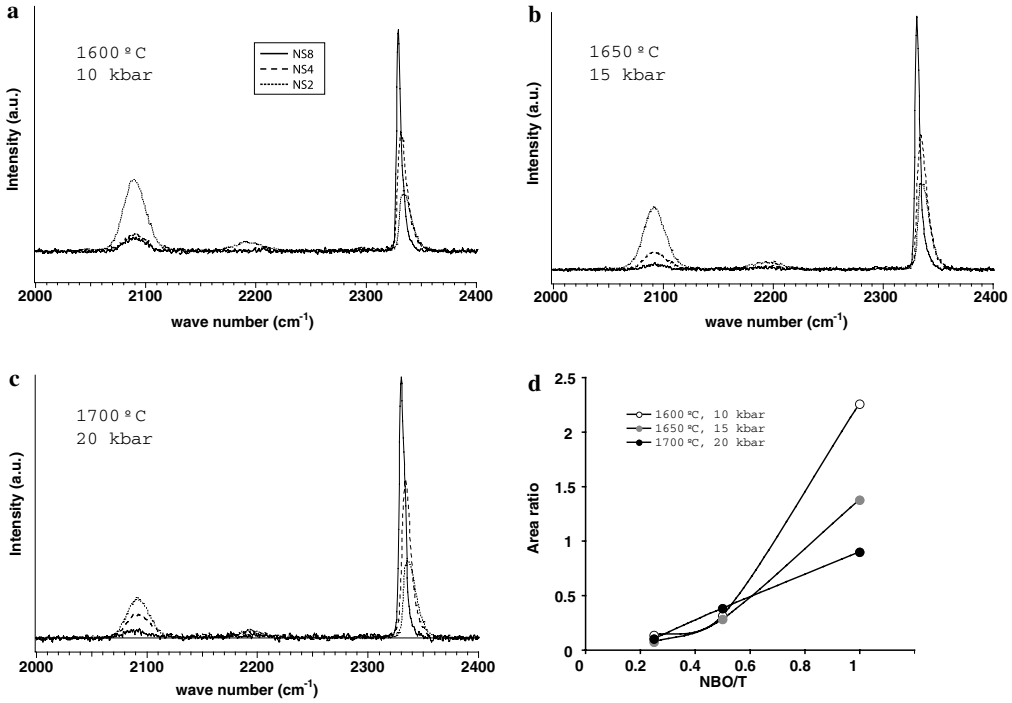

Fig. 8. Effect of the polymerization state of the liquid (quantified as NBO/T) on the high frequency region of Raman spectra of NS2, NS4, and NS8 glasses prepared under different experimental conditions (a, b, and c). (d) Ratio of the area below peaks at 2100 and 2300 cm^{-1} as a function of NBO/T for the different experimental conditions. Lines are only guides for the eyes.

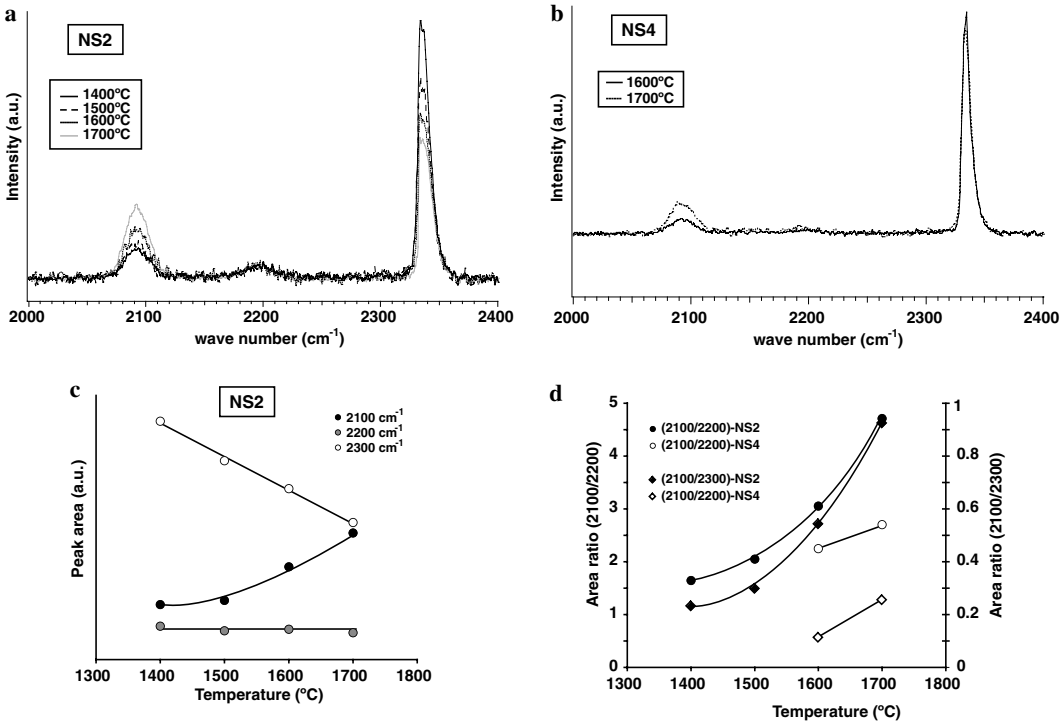

Fig. 9. Effect of temperature on the high frequency region of Raman spectra of NS2 (a) and NS4 (b) glasses prepared at 20 kbar. (c) Area below the three characteristic peaks for NS2. (d) Ratio of the area below peaks at 2100 and 2200 cm^{-1} and 2100 and 2300 cm^{-1} as a function of T for NS2 and NS4 glasses. Lines are only guides for the eyes.

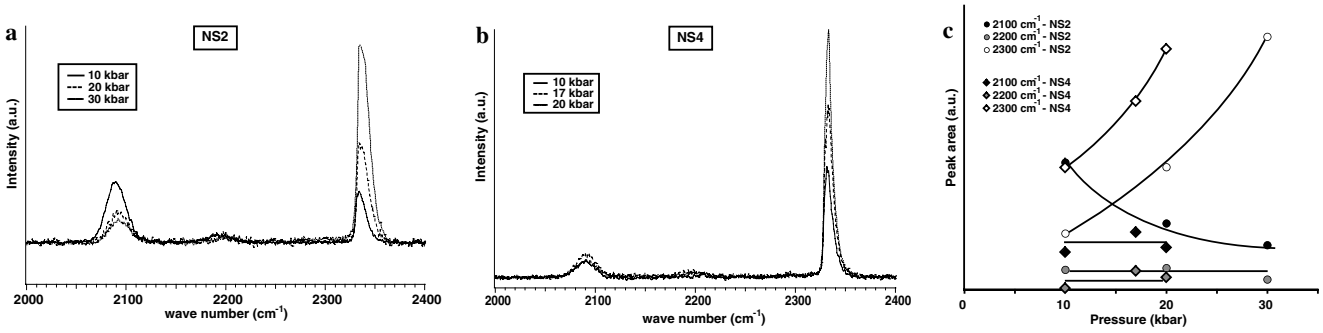

Fig. 10. Effect of pressure on the high frequency region of Raman spectra of NS2 (a) and NS4 (b) glasses prepared at 1600 °C. (c) Area below the three characteristic peaks for NS2 and NS4. Lines are only guides for the eyes.

is consistent with an increased distortion of the molecule as the silicate network is compressed. Pressure has no significant effect on peaks at 2100 and 2200 cm^{-1} except for NS2 at relatively low pressures are applied on NS2. In this case, increasing the pressure from 10 to 20 kbar results in a significant decrease of the intensity of the peak at 2100 cm^{-1}. Further pressure increase does not lead to any additional intensity decrease. Furthermore, such trend is not observed for NS4 glasses (Fig. 10c).

Pressure is thus required to form the chemical interaction between the melt and the volatile but once formed, further increase does not have a strong effect at least up to 30 kbar. However, as the content of molecular nitrogen increases rapidly, the overall relative content of this complex in the melt also increases.

3.3.6. A speciation typical of binary alkali liquids?

To quantify the behavior of nitrogen in silicate liquids further, potassium and lithium silicates have been synthesized (KS4 and LS4, respectively). Calcium, strontium, and barium silicates were prepared but as previously mentioned, only strontium silicate could be quenched from high pressure, high temperature experiments. Eventually a melt corresponding to the ambient pressure anorthite–diopside eutectic was studied (CMAS, Table 1).

Raman spectra of potassium-bearing melts exhibits two strong peaks around 2100 and 2200 cm^{-1}. Other parameters being equal, the relative intensities of these bands are higher for K- than for Na-bearing melts (Fig. 11a). Furthermore, these bands are shifted toward lower frequencies compared to their sodium counterparts. This is a strong

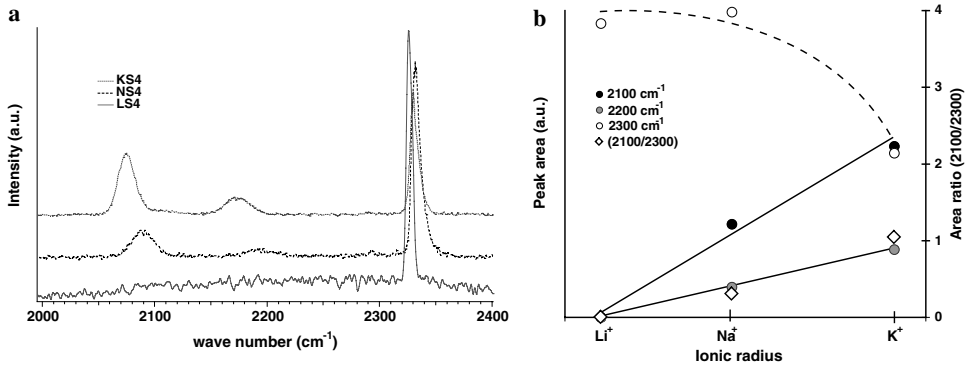

Fig. 11. Effect of the ionic radius on the high frequency region of Raman spectra of alkali silicate glasses prepared at 1600 °C and 17 kbar. Lines are only guides for the eyes.

indication that the local environment of this nitrogen species depends on the network-modifying cations. Conversely, Li-bearing silicates show a very different feature. In these melts nitrogen appears to dissolve exclusively as molecular nitrogen.

The areas below the different peaks are linear functions of the ionic radius of the alkali for bands 2100 and 2200 cm^{-1} (Fig. 11b). Conversely, the area below the peak of the molecular nitrogen is constant for Li- and Na-bearing silicates but decreases significantly for K-bearing glasses. These observations suggest that the presence of potassium (the largest of the three alkali cations studied) induces a significant decrease of the size of empty spaces within the structure. As a result, molecular nitrogen is less easily accommodated within the silicate melt structure. Correlatively, the intensity of the peak characteristic of nitrogen interacting with the silicate increases with the ionic radius of the network modifying cations. As discussed below, this link can be a consequence of the strength of M–O bonds or of the 'porosity' of the melt structure.

Raman spectra of alkaline-earth-bearing melts exhibits the band at 2100 cm^{-1} and in a lesser extend the peak at 2200 cm^{-1} (Fig. 12). For strontium silicates, this signal is dominant over that of the molecular nitrogen. It is thus obvious that the occurrence of a strong interaction between nitrogen and the silicate melt is not only typical of binary alkali silicates but is a common feature of silicate liquids. Other parameters being equal, the network modifying cation controls the speciation and the local environment of the dissolved nitrogen. This feature is observed not only in simple alkaline-earth binary melts but also in more complex $CaO–MgO–Al_2O_3–SiO_2$ melts.

4. Discussion

4.1. Insight into the nitrogen solubility at high pressure and high temperature

The present data can be used to address the effect of elevated pressure and temperature on the solubility of nitrogen in silicate melts. First, it must be noted that after the thermal decomposition of the silver azide, the gas mixture trapped into the capsule may be considered as pure nitrogen. The total pressure is thus comparable to the partial pressure of nitrogen.

The solubility of a volatile in silicate melts is usually described by a Henry's law. This approach is valid at low pressure and for species which have a nearly ideal behavior (e.g., noble gases and nitrogen). However, the fugacity coefficient (ΓN_2) of a given volatile is pressure-dependent. In our case, ΓN_2 may be calculated using a modified Redlich–Kwong equation of state using the critical constants for N_2 ($T_{crit} = 126.2$ K, $P_{crit} = 3.39$ MPa). At 1600 °C and for pressures of 1, 2, and 3 GPa, ΓN_2 is, respectively, 5.35, 29.63, and 164.82. Thus, at high-pressure, the usual assumption $fN_2 = PN_2$ is not correct. It explains why even

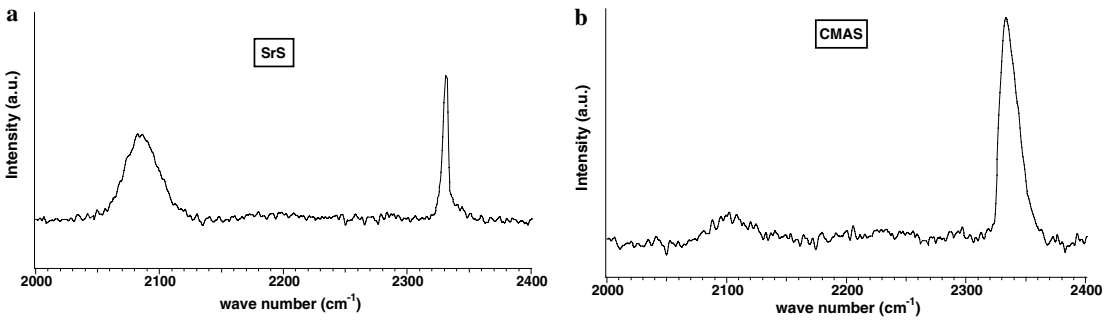

Fig. 12. Typical high frequency region of Raman spectra of strontium silicate (SrS) (a) and CMAS (b) glasses prepared at 1700 °C, 10 kbar and at 1600 °C, 20 kbar, respectively. Qualitatively the same features as in NS_x glasses are observed in these samples.

helium and neon solubility are not linear functions of their respective fugacity (Shelby, 1976). On the other hand, high-pressure noble gas solubility data show a linear pressure-dependence (Chamorro-Perez et al., 1996, 1998; Schmidt and Keppler, 2002; Bouhifd and Jephcoat, 2006). This paradoxical behavior has been explained recently (Sarda and Guillot, 2005). Though the solubility readily decreases when pressure increases, this effect is counterbalanced by the compression of the fluid phase. The Henrian behavior reported in experimental studies is thus only apparent. Nevertheless, it offers a unique and simple way to model and extrapolate experimental data to relatively high pressure. As a consequence, we have derived Henrian coefficient and we discuss these results below, keeping in mind that the Henrian behavior is only apparent.

For NS4, the nitrogen solubility follows an apparent Henry's law behavior within the error bars (Fig. 13). The Henry's constant is $9.23 \pm 1.3 \times 10^{-9}$ mol g^{-1} bar^{-1} at 1600 °C. This value is somewhat higher than values determined on synthetic melts studied at ambient pressure by Libourel et al. (2003) as well as values determined from natural basalts studied by Javoy and Pineau (1991) ($\sim 3.6 \times 10^{-9}$ mol g^{-1} bar^{-1}) and for natural basaltic melts equilibrated with air and studied by Marty (1995) ($3.7 \pm 1.1 \times 10^{-9}$ mol g^{-1} bar^{-1}). However, these results are still in reasonable agreement because the composition of the melt has a dramatic effect on the solubility of inert gases. For instance, the solubility of argon at 1–3 GPa pressures vary from about 3.44×10^{-9} mol g^{-1} bar^{-1} to more than 13×10^{-9} mol g^{-1} bar^{-1} as a function of the melt composition (Shibata et al., 1998; Schmidt and Keppler, 2002). A variation of more than one order of magnitude has also been observed in the case of N_2 solubility as a function of the melt composition at moderate pressure (Miyazaki et al., 2004). In addition to this compositional effect that is still difficult to take into account quantitatively, another bias may result from the fact that part of the nitrogen is not dissolved as an inert gas under high pressure. Nonetheless, this feature is probably not critical for NS4 glasses as demonstrated by the Henry's law behavior of nitrogen in this melt.

The solubility of nitrogen in NS2 does not follow any apparent Henry's law behavior, contrary to other volatiles at high pressure (Fig. 13). This was already indicated by the fact that the extrapolation of high pressure data to one bar pressure gives a nitrogen content of 0.1–0.2 wt% whereas experiments carried out at this pressure demonstrate that nitrogen solubility is below 0.1 ppm for a simplified MORB-like glass (Libourel et al., 2003). In other words, the solubility of nitrogen at high pressure in highly depolymerized liquids is not only a function of the nitrogen fugacity. This feature is likely due to the fact that a significant part of nitrogen is not dissolved in melts as an inert component. NMR data indicate that at least 15% of the nitrogen dissolved in NS2 at 20 kbar and 1600 °C is not as the molecular species. If this result is used to calibrate Raman spectra, the change of the relative fraction of nitrogen not dissolved as N_2 may be estimated for other experimental conditions (Fig. 13). At 10 kbar, this fraction is about 60% of the total nitrogen dissolved. The apparent excess of nitrogen measured in the melt, and consequently the apparent departure of the Henry's law behavior may then be quantitatively accounted for by this fraction of nitrogen which do not behave as an inert gas (Fig. 13).

Miyazaki (1996) showed that under oxidizing conditions, the solubility of nitrogen in the pressure range 1–800 bar followed Henry's law. This result has been extended recently by Libourel et al. (2003) and then by Miyazaki et al. (2004) to reducing conditions down to the IW buffer. Our results in part confirm these results to pressures up to 3 GPa provided that the melt is not highly depolymerized.

The NBO/T of NS4 is between mean andesite and mean tholeite melt values (Mysen and Richet, 2005). It can, thus, be expected that the solubility of nitrogen in such melts follows a Henry's law behavior at least up to 30 kbar. Under these conditions, the Henry's constant is identical to those

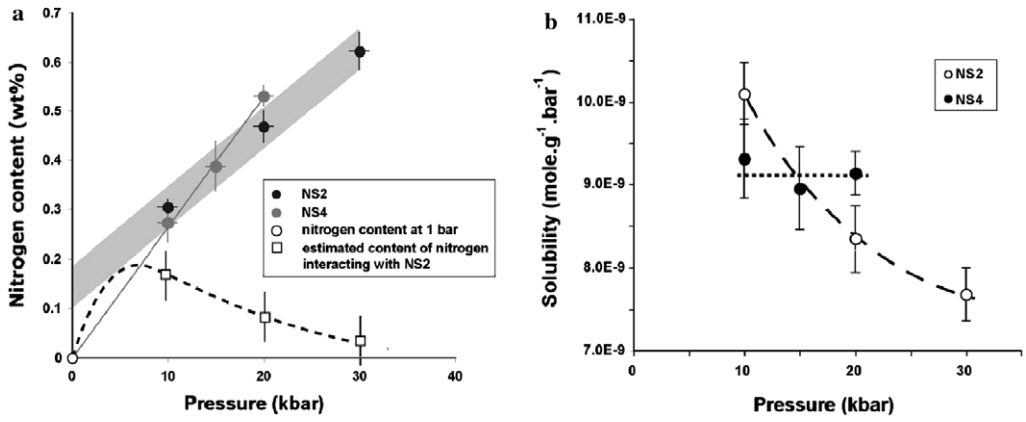

Fig. 13. (a) Nitrogen content of NS2 and NS4 glasses as a function of pressure. The extrapolation of the nitrogen content of NS2 glasses to ambient pressure gives anomalously high nitrogen content compared to experimental values (white dote, see text). This apparent excess may be explained by the presence of nitrosyl, the content of which has been determined using an empirical calibration of Raman spectra using NMR data (see text). (b) Nitrogen solubility as a function of pressure for NS2 and NS4. While NS4 exhibits a Henry's law behavior, NS2 clearly does not.

accurately determined experimentally up to few hundreds of atmospheres or measured on natural samples.

Turning now to the NS2 composition, the polymerization state is within the range of silica under-saturated basalts. For these liquids, the use of a Henry's law may lead to a significant underestimation of the nitrogen solubility. Finally, the situation is even more critical for the study of the degassing of a hypothetical magma ocean because those liquids are even more depolymerized than basalt.

4.2. Solubility mechanisms

The physical solubility of nitrogen (i.e., the dissolution of nitrogen as molecular N_2) and other inert gases have been described in several contributions (Doremus, 1966; Carroll and Stolper, 1991, 1993; Shibata et al., 1998; Schmidt and Keppler, 2002). It may be simply written as:

$$N_{2(gas)} = N_{2(melt)} \quad (3)$$

Qualitatively, this reaction is similar to that which describes the dissolution of noble gases. It thus depends on the number and the size of empty spaces existing within the melt structure. Our results are in agreement with this description. More interestingly, the fact that molecular nitrogen is a simple diatomic molecule can be used to illustrate the effect of composition and pressure on the 'ionic porosity' of the melt. Indeed, silica-rich, polymerized melts are supposed to have a larger 'ionic porosity' than other, less polymerized glasses (Shelby, 1976; Carroll and Stolper, 1991). Therefore, the nitrogen solubility should be higher. This is actually observed experimentally (Figs. 2 and 8).

The local environment of N_2 changes continuously, however, from polymerized to depolymerized liquids. It is significantly more distorted in the latter case as demonstrated by the broadening and the frequency shift of the N_2 vibron (Fig. 8). The effect of pressure on the local environment is also consistent with the distortion of the molecule as the silicate network is squeezed (Fig. 10). Given this increasing distortion of the N_2 molecule, the loss of the inert behavior as a function of pressure becomes a critical question.

It is likely that previous models describing the solubility of noble gases in silicates may be applied to the behavior of the fraction of nitrogen dissolved as a molecular species. Nevertheless, the effect of pressure on this mechanism (and thus the way models take this parameter into account) is still discussed. High-pressure data on noble gases solubilities show a contrasted picture. It is, for instance, not clear if their solubility reaches a plateau at a given pressure, generally higher than 50 kbar (and thus beyond the pressure range considered in this study) or drops abruptly (Chamorro-Perez et al., 1996, 1998; Schmidt and Keppler, 2002). Based on the significant change in Raman frequency and shape of the N_2 vibron, one may anticipate that a progressive collapse of the silicate structure could affect the dissolution of nitrogen at very high pressure.

More important, but still hypothetical, is the mechanism that leads part of the nitrogen to interact chemically with the network. Under highly reducing conditions it has been demonstrated (e.g., Mulfinger, 1966) that part of the nitrogen is chemically bonded to the silicate by forming nitrides (N^{3-} groups). However, our Raman and NMR data indicate that such process is not at work in our samples and that nitrosyl groups are the most likely group that form in melts at high pressure and high temperature.

Addressing now the formation of such species, we note that the fraction of this species is larger in depolymerized liquids. In addition, the nature of the network modifying cation affects the characteristic frequency and intensity of Raman band assigned to vibrations of bonds in this species. It is thus likely that nitrogen does not react with bridging oxygen but with non-bridging oxygen. Interestingly, the relative concentration of this species is correlated with the ionic radius of the network-modifying cation. The larger the cation, the larger is the relative content. One possible explanation may be found in a different strength of the M–O bonds or in a different degree of ionicity of these bonds. However, these differences are relatively small and unlikely account for the very contrasted behavior of nitrogen in MS4 glasses, for example. Another usual scaling parameter is the electronegativity scale or the mixing enthalpy scale (Hess, 1995). However, if these parameters were relevant, it would not be expected to find nitrosyl groups in calcium–magnesium aluminosilicate and in strontium silicate glasses because the sequences are $K > Na > Ba > Li > Sr > Ca > Mg$ and $K > Na > Ba > Sr > Li > Ca > Mg$, respectively. The only sequence that reproduces the trends observed is the ionic radius of the cations. This leads to the conclusion that the formation of nitrosyl groups is in part controlled by a steric effect. The larger the cation, the less porous the silicate network and the more prevalent is the nitrosyl groups.

Nevertheless, a simple process that leads to the formation of nitrosyl starting from N_2 is difficult because nitrogen has to be partially oxidized. The fact that nitrosyl is found in glasses loaded under an argon flow tends to rule out the direct effect of molecular oxygen from air trapped in the sealed sample containers. Thus, the oxidation may be explained either by an electron loss through the platinum capsule or by a reaction involving water. In the former case, it is well known that water trapped in the talc furnace parts dissociates into OH^- and H^+ at high pressure and temperature. In this way, a limited charge transfer, involving H^+ as an electron acceptor, could occur during the experimental run.

Another way to oxidize nitrogen is to involve H_2O directly. Water was not detected by Raman spectroscopy and thus if present its content should not exceed few 0.1 wt%. Nevertheless, it is nearly impossible to study strictly anhydrous compositions at high pressure (see, for example, Eggler and Kadik, 1979). Preliminary results on water-bearing compositions indicate that a detectable level of water in NS4 promotes the formation of ammonium

complexes, but at low content, nitrosyl and ammonium coexist in glasses (unpublished data). Thus, it is possible that a small amount of water, probably adsorbed at the surface of the azide promote the formation of nitrosyl. If water is involved in the reaction path, a simple equation can account for the features detailed above:

$$2\text{Si–O–Na} + \text{N}_2 + 2\text{H}_2\text{O} = 2\text{Si–O–N} + \text{H}_2 + 2\text{NaOH} \quad (4)$$

This reaction accounts for the moderately oxidized state of nitrogen, the role of non-bridging oxygens and the effect of modifying cation on the environment of the nitrogen within the glass. The total amount of water required to form nitrosyl is small and cannot be measured with available

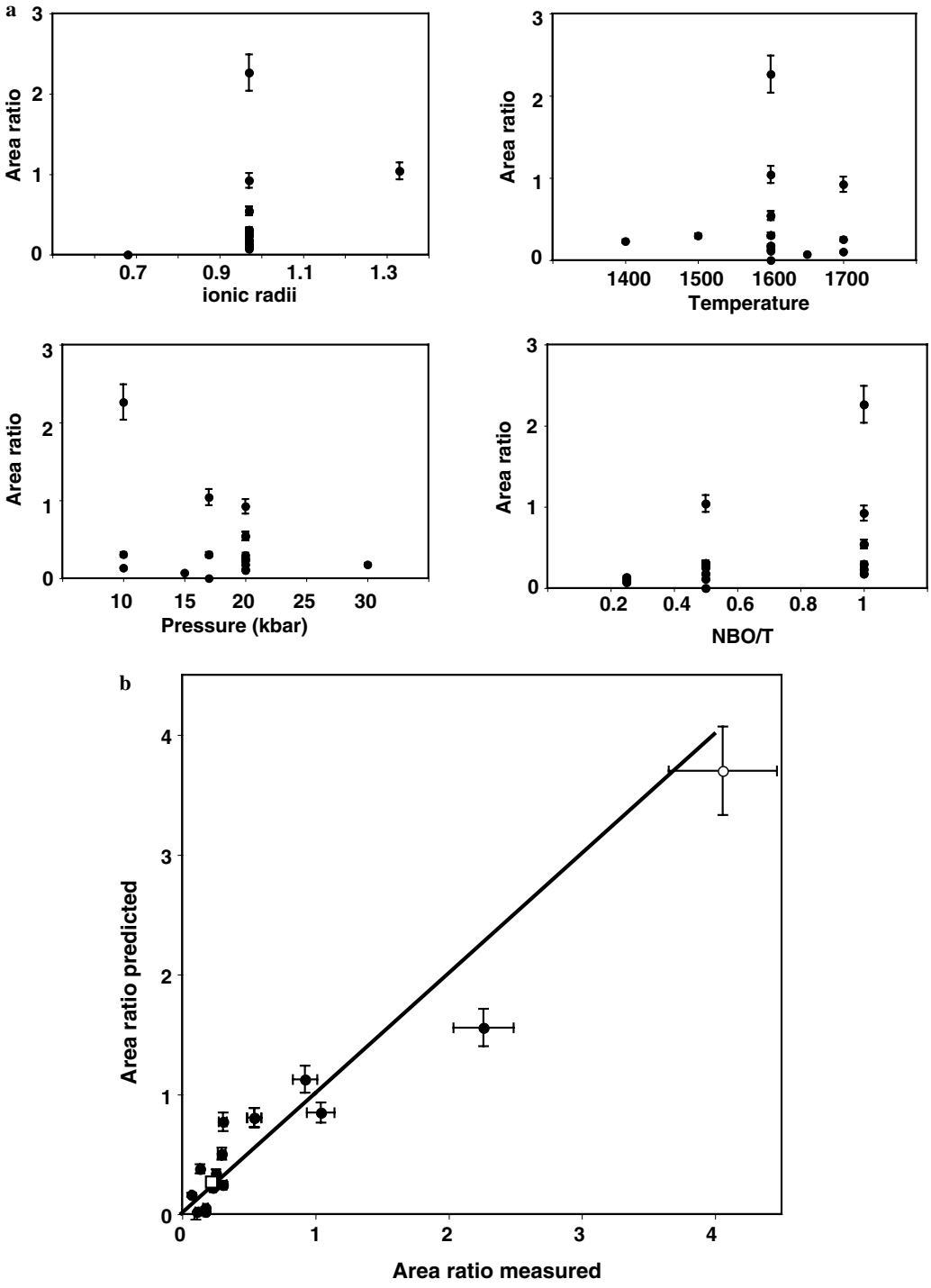

Fig. 14. (a) 2D representation of the data used to determine the empirical relationship between the ratio of area below peaks at 2100 and 2300 cm^{-1} and P, T, and X parameters. (b) Measured and predicted values of the ratio. The line corresponds to the expected 1:1 correlation between both values. Black dotes correspond to the data used to determine the multi-variant fit. White dotes correspond to calculated values of the ratio for CMAS (low value) and SrS (high value) glasses using the empirical relationship. Indicative error bars have been settled to ±10%.

analytical methods. Given the molecular weight of N_2 and H_2O, the water content required to oxidize a few 0.1 wt% of nitrogen is still below the detection limit. This reaction path is, nevertheless, still hypothetical.

4.3. First attempt to determine the P–T–X dependence of the nitrogen speciation in silicate melts

Experimental data cover a relatively large range of composition, pressure and temperature conditions (Fig. 14a). Therefore, they may be used to determine an empirical equation quantifying the P–T–X dependences of the nitrogen speciation in silicate liquids. For this purpose, we used the ratio of areas below peaks at 2100 and 2300 cm^{-1}, which embody NO and N_2 species, respectively. As described previously, the individual P, T, X-dependence of this speciation is probably not linear but given the number of independent parameters involved in this equation, we generally assumed linear dependence. A notable exception in this respect is the effect of temperature, which is expressed as a function of T^2 to account for the clear non-linear T-dependence (Fig. 9). A multi-variant equation has been fitted to all the data collected for binary alkali melts. The equation is of the form

$$R_{NO/N_2} = k_0 + k_1 \cdot \frac{nbo}{t} + k_2 \cdot r + k_3 \cdot P + k_4 \cdot T^2, \quad (5)$$

where R_{NO/N_2} is the ratio of the area below the peaks of interest, nbo/t is the number of non-bridging oxygen per tetrahedron, r is the ionic radius of network modifying cation, P is the pressure in kilobar, T is the temperature in degree Celsius, and k_0, k_1, k_2, k_3, and k_4 are the parameters of the equation and are given in Table 4.

Predicted and measured values are in good agreement given the accuracy of spectroscopic methods available to quantify the speciation of nitrogen (Fig. 14b). More importantly, we applied this equation to melts very different from those used to derive Eq. (5). Predicted values of the relative content of the different species dissolved in CMAS and SrS liquids have been determined. For CMAS melts, a mean ionic radius was used to account for the presence of both calcium and magnesium. The nbo/t was calculated by considering that all the aluminum was tetrahedrally coordinated. Furthermore, these two liquids exhibit very different relative Raman intensities (Fig. 12) and have been synthesized under very different conditions. For these dramatically different melts, Eq. (5) reproduces well the measured values within a 10% uncertainty (Fig. 14b). Though purely empirical, this equation may thus be applied to liquids having very different compositions and polymerization states. However, the extrapolation of the equation to much higher temperature and pressure may be questionable especially because of the change of the coordination number of silicon and aluminum at very high pressure. For instance, it is well known that above 15 GPa, silicon coordination number change progressively from four to six (Hemley et al., 1986, 1994; Williams et al., 1993). The effect of this transition on the nitrogen solubility behavior has however still to be studied.

Table 4
Parameters of Eq. (5) determined by a multi-variant fit to experimental data

k_0	-3.377 ± 1.22
k_1	1.571 ± 0.295
k_2	1.674 ± 0.654
k_3	-0.0752 ± 0.017
k_4	$9.72e{-}07 \pm 3.74e{-}07$

5. Concluding remarks

The behavior of nitrogen in deep geochemical reservoirs is generally inferred from its similarity with noble gases. This study indicates that this assumption is not completely true at high pressure. Under very reducing conditions, nitrides are probably the main speciation of nitrogen as shown in several studies. The stability of such compounds extends to pressures typically relevant for the Earth core (Adler and Williams, 2005). Under more oxidizing conditions, nitrosyl may represent a significant part of the nitrogen dissolved and above a still undetermined content of water it is likely that ammonium also coexist with molecular nitrogen. The formation of nitrosyl is responsible for an apparent deviation from the Henry's law behavior. Furthermore, this deviation as well as the relative content of the nitrosyl species may be roughly quantified.

Another critical question that arises from this study is the real partitioning behavior of these nitrogen-bearing groups between melt and crystals. This parameter strongly controls degassing processes and the real nitrogen content of geochemical reservoirs. It is commonly assumed that partitioning coefficient of nitrogen between melts and crystals may be approximated in the light of the partitioning behavior of noble gases (Brooker et al., 2003). Then, according to existing models such as the 'lattice strength model' (Brice, 1975; Blundy and Wood, 1994), nitrogen must be a very incompatible element. This theory is based on the ionic (or atomic or molecular) size of the element of interest and its electrical property. In this respect, N_2, because of its zero-charge and its size must be very incompatible. However, nitrosyl, ammonium, and nitride complexes in melts have no reason to behave like noble gases. Thus, part of the nitrogen initially dissolved in a putative Hadean magma ocean or in any kind of deep magma chamber may not be as incompatible as previously assumed.

Finally, turning to a hypothetical isotopic fractionation of nitrogen, it has been shown in the case of water that decompression of a magma may lead to a significant fractionation of the D/H ratio (Pineau et al., 1998). This is likely induced by the dual speciation of water in silicate melts (as molecular water and OH groups). Our study shows that the behavior of nitrogen under high pressure is closer to that of water than to that of noble gases. Thus, the question of a potential isotope fractionation of nitrogen during a degassing event must be envisaged.

Acknowledgments

The Carnegie Institution of Washington supported this work. We thank Chris Hadidiacos for the help provided during electron microprobe analyses. Reika Yokochi and Vincent Busigny are also thanked for thoughtful comments. We thank the W. M. Keck Foundation, the NSF, and the Carnegie Institution for support of the W. M. Keck Solid State NMR findings. We thank M. A. Bouhifd and an anonymous reviewer for very helpful and constructive reviews.

Associate editor: Claudia Romano

References

Adler, J.F., Williams, Q., 2005. A high-pressure X-ray diffraction study of iron nitrides: implications for the Earth's core. *J. Geophys. Res.* **110**, B01203.

Blundy, J.D., Wood, B.J., 1994. Prediction of crystal–melt partition coefficients from elastic moduli. *Nature* **372**, 452–454.

Bouhifd, M.A., Jephcoat, A.P., 2006. Aluminium control of argon solubility in silicate melts under pressure. *Nature* **439**, 961–964.

Boyd, F.R., England, J.L., 1960. Apparatus for phase equilibrium measurements at pressures up to 50 kb and temperatures up to 1750 °C. *J. Geophys. Res.* **65**, 741–748.

Brice, J.C., 1975. Some thermodynamics aspects of the growth of strained crystals. *J. Cryst. Growth* **28**, 249–253.

Broadhurst, C.L., Drake, M.J., Hagee, B.E., Bernatowicz, T.J., 1992. Solubility and partitioning of Ne, Ar, Kr, and Xe in minerals and synthetic basalt melts. *Geochim. Cosmochim. Acta* **56**, 709–723.

Brooker, R.A., Du, Z., Blundy, J.D., Kelley, S.P., Allan, N.L., Wood, B.J., Chamorro, E.M., Wartho, J.-A., Purton, J.A., 2003. The 'zero-charge' partitioning behaviour of noble gases during mantle melting. *Nature* **423**, 738–741.

Brooker, R.A., Wartho, J.-A., Carrol, M.R., Kelley, S.P., Draper, D.S., 1998. Preliminary UVLAMP determinations of argon partition coefficient for olivine and clinopyroxene grown from silicate melts. *Chem. Geol.* **147**, 185–200.

Canil, D., 2002. Vanadium in peridotites, mantle redox and tectonic environments: Archean to present. *Earth Planet. Sci. Lett.* **195**, 75–90.

Carroll, M.R., Stolper, E.M., 1991. Argon solubility and diffusion in silica glass: implication for the solution behavior of molecular gases. *Geochim. Cosmochim. Acta* **55**, 211–226.

Carroll, M.R., Stolper, E.M., 1993. Noble gas solubilities in silicate melts and glasses: new experimental results for argon and the relationship between solubility and ionic porosity. *Geochim. Cosmochim. Acta* **57**, 5039–5052.

Chamorro-Perez, E.M., Gillet, P., Jambon, A., 1996. Argon solubility in silicate melts at very high pressures: experimental set-up and preliminary results for silica and anorthite melts. *Earth Planet. Sci. Lett.* **145**, 97–107.

Chamorro-Perez, E.M., Gillet, P., Jambon, A., Badro, J., McMillan, P., 1998. Low argon solubility in silicate melts at high-pressure. *Nature* **393**, 352–355.

Dickinson, J.E., Scarfe, C.M., McMillan, P., 1990. Physical properties and structure of $K_2Si_4O_9$ melt quenched from pressure up to 2.4 GPa. *J. Geophys. Res.* **95**, 15675–15681.

Doremus, R.H., 1966. Physical solubility of gases in fused silicates. *J. Am. Ceram. Soc.* **49**, 461–462.

Eggler, D.H., Kadik, A.A., 1979. The system $NaAlSi_3O_8$–H_2O–CO_2 to 20 kbar pressure: I. Compositional and thermodynamic relations of liquids and vapors coexisting with albite. *Am. Miner.* **64**, 1036–1048.

Grande, T., Jacob, S., Holloway, J.R., McMillan, P.F., Angell, C.A., 1995. High-pressure synthesis of nitride glasses. *J. Non-Cryst. Solids* **184**, 151–154.

Gregoryanz, E., Sanloup, C., Somayazulu, M., Badro, J., Fiquet, G., Mao, H.-K., Hemley, R.J., 2004. Synthesis and characterization of a binary noble metal nitride. *Nat. Mater.* **3**, 294–297.

Hashizume, K., Chaussidon, M., Marty, B., Robert, F., 2000. Solar wind record on the moon: deciphering presoler from planetary nitrogen. *Science* **290**, 1142–1145.

Hemley, R.J., Mao, H.-K., Bell, P.M., Mysen, B.O., 1986. Raman spectroscopy of SiO_2 glass at high pressure. *Phys. Rev. Lett.* **57**, 747–750.

Hemley, R.J., Prewitt, C.T., Kingma, K.J., 1994. High-pressure behavior of silica. In: Heaney, P.J., Prewitt, C.T., Gibbs, G.V. (Eds.), *Silica: Physical Behavior, Geochemistry and Materials properties*. Mineralogical Society of America, Washington, DC, pp. 41–82.

Hess, P.C., 1995. Thermodynamic mixing properties and the structure of silicate melts. In: Stebbins, J.F., McMillan, P.F., Dingwell, D.B. (Eds.), *Structure, Dynamics and Properties of Silicate Melts*. Mineralogical Society of America, Washington, DC, pp. 145–189.

Hiyagon, H., Ozima, M., 1986. Partition of rare gases between olivine and basalt melt. *Geochim. Cosmochim. Acta* **50**, 2045–2057.

Holloway, J.R., Reese, R.L., 1974. The generation of N_2–CO_2–H_2O fluids for use in hydrothermal experimentation. I. Experimental method and equilibrium calculations in the C–O–H–N system. *Am. Mineral.* **59**, 587–597.

Jambon, A., Weber, H., Braun, O., 1986. Solubilities of He, Ne, Ar, Kr and Xe in a basalts melt in the range 1250–1600 °C. *Geochim. Cosmochim. Acta* **50**, 401–408.

Jameson, C.J., Jameson, A.K., Wille, S., Burell, P.M., 1981. Variation of chemical shielding with intermolecular interaction and rovibrational motion. V. ^{15}N in N_2. *J. Chem. Phys.* **74**, 853–856.

Javoy, M., 1997. The major volatile elements of the Earth: their origin, behavior, and fate. *Geophys. Res. Lett.* **24**, 177–180.

Javoy, M., Pineau, F., 1991. The volatile record of a popping rock from the mid-Atlantic ridge at 14°N: chemical and isotopic composition of gases trapped in the vesicles. *Earth Planet. Sci. Lett.* **107**, 598–611.

Keppler, H., 1989. A new method for the generation of N_2-containing fluids in high-pressure experiments. *Eur. J. Mineral.* **1**, 135–137.

Kirsten, T., 1968. Incorporation of rare gases in solidifying enstatite melts. *J. Geophys. Res.* **73**, 2807–2810.

Libourel, G., Marty, B., Humbert, F., 2003. Nitrogen solubility in basaltic melt. Part I. Effect of oxygen fugacity. *Geochim. Cosmochim. Acta* **67**, 4123–4135.

Lux, G., 1986. The behaviour of noble gases in silicate liquids: solution, diffusion, bubbles and surface effects, with applications to natural samples. *Geochim. Cosmochim. Acta* **51**, 1549–1560.

Long, D.A., 1977. *Raman Spectroscopy*. McGraw-Hill, New York.

Maekawa, H., Maekawa, T., Kawamura, K., Yokokawa, T., 1991. The structural groups of alkali silicate glasses determined from ^{29}Si MAS-NMR. *J. Non-Cryst. Solids* **127**, 53–64.

Marty, B., 1995. Nitrogen content of the mantle inferred from N_2–Ar correlation in oceanic basalts. *Nature* **377**, 326–329.

Marty, B., Dauphas, N., 2003. The nitrogen record of crust–mantle interaction and mantle convection from Archean to present. *Earth Planet. Sci. Lett.* **206**, 397–410.

McMillan, P.F., Sato, R.K., Poe, B.T., 1998. Structural characterization of Si–Al–O–N glasses. *J. Non-Cryst. Solids* **224**, 267–276.

Miyazaki, A., 1996. Studies on Solubilities of Nitrogen and Noble Gases in Silicate Melts. Ph.D. dissertation University of Tokyo.

Miyazaki, A., Hiyagon, H., Sugiura, N., 1995. solubility of nitrogen and argon in basalt melt under oxidizing condition. In: K.A. Farley (Ed.), Volatiles in the Earth and Solar System, pp. 276–283.

Miyazaki, A., Hiyagon, H., Sugiura, N., Hirose, K., Takahashi, E., 2004. Solubilities of nitrogen and noble gases in silicate melts under various oxygen fugacities: implications for the origin and degassing history of nitrogen and noble gases in the Earth. *Geochim. Cosmochim. Acta* **68**, 387–401.

Mulfinger, H.O., 1966. Physical and chemical solubility of nitrogen in glass melts. *J. Am. Ceram. Soc.* **49**, 462–467.

Mysen, B.O., 1990. Effect of pressure, temperature, and bulk composition on the structure and species distribution in depolymerized alkali aluminosilicate melts and quenched melts. *J. Geophys. Res.* **95**, 15733–15744.

Mysen, B.O., Richet, P., 2005. *Silicate Glasses and Melts: Properties and Structure*. Elsevier, Amsterdam.

Navarro, J.M.F., 1998. Oxynitride glasses. *Glastech. Ber. Glass Sci. Technol.* **71**, 263–276.

Pineau, F., Shilobreeva, S., Kadik, A., Javoy, M., 1998. Water solubility and D/H fractionation in the system basaltic andesite–H_2O at 1250 °C and between 0.5 and 3 kbars. *Chem. Geol.* **147**, 173–184.

Rouxel, T., Piriou, B., 1996. Free silicon and crystallization in silicon nitride based ceramics and in oxynitride glasses. *J. Appl. Phys.* **79**, 9074–9079.

Rouxel, T., Besson, J.-L., Rzepka, E., Goursat, P., 1990. Raman spectra of SiYAlON glasses and ceramics. *J. Non-Cryst. Solids* **122**, 298–304.

Sakka, S., 1995. Structure, properties and application of oxynitride glasses. *J. Non-Cryst. Solids* **181**, 215–224.

Sanloup, C., Hemley, R.J., Mao, H.-K., 2002. Evidence for xenon silicates at high pressure and temperature. *Geophys. Res. Lett.* **29**.

Sarda, P., Guillot, B., 2005. Breaking of Henry's law for noble gases and CO_2 solubility in silicate melts under pressure. *Nature* **436**, 95–98.

Schmidt, B.C., Keppler, H., 2002. Experimental evidence for high noble gas solubilities in silicate melts under mantle pressures. *Earth Planet. Sci. Lett.* **195**, 277–290.

Shelby, J.E., 1976. Pressure dependence of helium and neon solubility in vitreous silica. *J. Appl. Phys.* **47**, 135–139.

Shibata, T., Takahashi, E., Matsuda, J.I., 1998. Solubility of neon, argon, krypton and xenon in binary and ternary silicate systems: a new view on noble gas solubility. *Geochim. Cosmochim. Acta* **62**, 1241–1253.

Tolstikhin, I.N., Marty, B., 1998. The evolution of terrestrial volatiles: a view from helium, neon, argon and nitrogen isotope modeling. *Chem. Geol.* **147**, 27–52.

Williams, Q., Hemley, R.J., Kruger, M.B., Jeanloz, R., 1993. High-pressure infrared spectra of α-quartz, coesite, stishovote and silica glass. *J. Geophys. Res.* **93**, 2280–2288.

Xue, X., Stebbins, J.F., Kanzaki, M., Tronnes, R., 1989. Silicon coordination and speciation changes in a silicate liquid at high pressures. *Science* **245**, 962–964.